J Mater Sci: Mater Med (2010) 21:685–694
DOI 10.1007/s10856-009-3902-2

In vitro bioactivity of sol–gel-derived hydroxyapatite particulate nanofiber modified titanium

Madhab Prasad Bajgai · Daman Chandra Parajuli · Soo-Jin Park · Kong Hee Chu · Hyung-Sub Kang · Hak Yong Kim

Received: 4 May 2009 / Accepted: 5 October 2009 / Published online: 23 October 2009

Abstract A chemically-etched titanium surface was modified by electrospinning a sol–gel-derived hydroxyapatite (HAp) that was subjected to calcination within the temperature range of 200–1400°C in the normative atmospheric condition. After heat treatment, crystal structures of the filmed titanium oxide and HAp on the titanium's surface were identified using wide-angle X-ray diffraction. A highly porous layer of HAp was found to have formed on the oxidized titanium surfaces. The surfaces of three different samples; (1) electrospun HAp, (2) HAp calcined at 600°C, and (3) HAp calcined at 800°C, were investigated for their ability to foster promotion, proliferation, and differentiation of human osteoblasts (HOB) (in the 9th passage) in vitro up to 6 days. Among the three samples, cells cultured on the HAp calcined at 800°C titanium surfaces displayed the best results with regard to adhesion, growth, and proliferation of HOB. This novel method for fabrication of titanium substrates would provide a promising improvement for titanium-based medical devices over the current standards, which lack such substrates. These titanium substrates explicitly provide enhanced HOB proliferation in terms of both desired surface properties and their produced bulk quantity.

M. P. Bajgai · D. C. Parajuli
Department of Bionanosystem Engineering, Chonbuk National University, Jeonju 561-756, Republic of Korea

S.-J. Park
Center for Healthcare Technology Development, Chonbuk National University, Jeonju 561-756, Republic of Korea

K. H. Chu
Clean and science Co., Ltd, Samsung Dong, Kangnam Ku, Seoul, Republic of Korea

H.-S. Kang
College of Veterinary Medicine, Chonbuk National University, Jeonju 561-756, Republic of Korea

K. H. Chu · H. Y. Kim (✉)
Department of Textile Engineering, Chonbuk National University, Jeonju 561-756, Republic of Korea
e-mail: Khy@chonbuk.ac.kr

1 Introduction

The key characteristics of any given biomaterial, such as non-toxicity, corrosion resistance, modulus of elasticity, and fatigue strength are important factors to consider in any specific biomedical application. Metals and metal alloys such as grade 316L stainless steel, cobalt-based alloys, and titanium (Ti) alloys are frequently used as implant materials for bone plates, screws, and hip joint prostheses [1]. While the typical grade 316L stainless steel is stronger and cheaper than other alloys, its corrosion properties and propensity to provoke infection renders it inferior to Ti-based alloys. On the other hand, cobalt-based alloys cast better and have sufficient strength to withstand occlusal forces applied to partial denture frameworks, a common application of biomaterials. These cobalt-based alloys exhibit reasonable biodegradation properties when exposed to human tissues, but are not as resistant to corrosion as Ti. These alloys are frequently used to fabricate hip prostheses [1, 2].

In relation to materials suitable for implant, Ti and Ti alloys are highly regarded as skeletally appropriate biomaterials because of their good biocompatibility and relative bioinertness [1]. Specifically, commercially pure Ti (CP, Ti) is lightweight, corrosion resistance, has reasonable formability, and possesses suitable strength-to-weight ratio. This material also allows direct bone-to-implant contact, also called "osseointegration". In addition, Ti imparts forces

to the bone not only due to its low modulus of elasticity but also due to its high tensile strength, which is comparable to carbon steel [3]. Unfortunately, like most metals, Ti exhibits poor bioactive properties [4, 5]. A bioinert material, which is stable in the human body and does not react with bodily fluids and tissues, is generally encapsulated after its implantation into the living body by fibrous tissues that isolate the material from the surrounding bone. The biological tissues typically interact with the outermost atomic layers of an implant, therefore, placing heavy importance on the implant material's surface properties with respect to possible tissue exposure reactions and osteoconductivity [5–7]. In this respect, Ti, with its bio-inert surface, has difficultly achieving a sufficient chemical bond with skeletal bone and, during the early stage immediately following implantation, has difficulty forming new bone tissue on its surface. Hence, Ti and Ti alloys do not meet all the requirements of the 'ideal' biomaterial [8]. Thus, there is an urgent need for surface modification of normally bioinert materials with properly bioactive materials. Although Ti oxide formed on the surface may act as a bioactive material, however, such an oxidized layer is easily contaminated by hydrocarbons or other elements when exposed to a non-sterile environments, e.g., immersion in biological fluids. Meanwhile, electrochemically prepared oxides may also contain some impurities due to anion incorporation from the electrolytes used, such as Cl, S, Si, P, and Na [9].

During the past several decades, numerous surface modification techniques aimed at improving biocompatibility of an implant's surface have been proposed. These techniques attempt to improve the biocompatibility of the implant surface by altering surface topography, physical characteristics, or chemical properties of Ti. Such techniques include abrasion, sand-blasting, acid etching, electrochemical oxidation, or combinations thereof. HAp, the most ubiquitous ingredient within the family of bioceramic constructions, is attractive in such a way that it mimics both the mineral composition and porous structure of the bone. Moreover, it also forms a direct bond with the neighboring bone tissues because of its ability to induce differentiation of mesenchymal cells into osteoblastic cells [9, 10]. Although ceramics alone have excellent corrosion resistance and good bioactive properties, porous ceramic structures are limited to non-load-bearing applications. This limitation is due to their intrinsic brittleness that results in low toughness and low flexural strength [11–13]. Meanwhile, metallic implant surfaces modified with bioactive materials like HAp have shown good fixation to the host bone. Apatite formation is currently believed to be the main requirement for the bone-bonding ability of materials [5].

Thermal oxidation can form an outer "ceramic" layer of rutile on Ti surface [9]. Feng et al. [14] reported that thermal treatment of Ti in a different atmosphere could alter surface chemical composition, surface roughness, surface energy, and perhaps even improve osteoblast responses to the resulting modified Ti surfaces. Various physical and chemical treatments of the Ti surface have been proposed with an aim of obtaining a most biocompatible implant surface. Included among the techniques found to be beneficial for the biological performance of implants is increasing the surface roughness, the oxidation of Ti to form a TiO_2 layer on the surface, and the incorporation of Ca or P ions into the surface layer. The validity of these results has been confirmed by several different researchers [15, 16]. The most widely used commercial techniques to accomplish these methods are sandblasting, acid etching, and plasma spraying of HAp [6, 7]. We investigated the effects on the surface modification of Ti using the sol–gel-derived electrolytic precursor with successive calcinations. Thus we obtained nano-topographical matrices, which were subjected to biocompatibility test using HOB [1, 2].

The present work confirms the first successful surface modification of Ti with HAp particulate nanofibers using a simple electrospinning method. Furthermore, HOB attachment and proliferation on electrospun Ti surfaces followed by calcinations at different temperature ranges (from 200 to 1400°C at 200°C intervals) were examined. Such a surface modification of Ti nano-architectures by sol–gel-derived HAp nanofibers are cost-effective, enabling realization of desired platform topologies on existing unmodified implant materials.

2 Materials and methods

2.1 Materials

Commercially available pure Ti (CP, Ti, Grade 2, Ka-Hee Metal Industry Co., Korea), machined into disks ($10 \times 10 \times 2$ mm^3) was used as the substrate. These disks were ground using 1200-grit silicon carbide sandpaper and cleaned ultrasonically in acetone and deionized water. The samples were then pickled using a mixture of hydrogen peroxide (H_2O_2) and sulfuric acid (H_2SO_4) in the ratio of 1:1 by volume for 50 s and subsequently washed in distilled water. The substrates were dried in a vacuum before using for electrospinning. Calcium glycerol phosphate (Ca-GP), calcium acetate (Ca-Ac), and all the reagents were purchased from Sigma–Aldrich Co., USA, and used without further purification. Polyvinyl alcohol (PVA, $M_w = 65{,}000$ Daltons) was purchased from Dong Yang Chem. Co., Korea. HOB cell line CCRL-11372 was purchased from ATCC, USA. All culture media, reagents and buffer constituents were purchased from Gibco Co., USA.

2.2 Electrospinning

The electrospinning setup employed in this study was similar to that reported in previous work [17, 18]. In a typical experiment, homogeneous aqueous slurry of Ca-GP and Ca-Ac with Ca/P ratio 1.67 was treated with 9% (w/w) PVA (aqueous) solution in the ratio of 3:7 by weight to get a clear sol–gel, and electrospun by applying 15 kV at an electrode distance of 15 cm. The fibers were collected on Ti disks (chemically etched and dried) and subjected to calcination at various temperatures ranging from 200 to 1400°C. A Ti disk that is electrospun but not calcined is referred to as Ti-HAp, whereas the disks that are electrospun and calcined at temperatures ranging 200–1400°C are referred to as Ti-HAp 200, Ti-HAp 400, etc.

2.3 Characterization

Fourier transform infrared spectra (FT-IR) of the samples were recorded by the ATR-FTIR method using an ABB Bomen MB100 Spectrometer (Bomen Inc., Canada). Crystallographic patterns were acquired at room temperature using wide-angle X-ray diffraction (WAXD) with Cu-Kα radiation, operated at 40 kV and 30 mA. The patterns were acquired over a diffraction angle of $2\theta = 10$–$80°$. The morphology of the HAp particulate nanofiber was examined using FE-SEM (S-4700, Hitachi CO., Japan) at an accelerating voltage of 10 kV after a plasma coating of the specimens with OsO_4. Further, the morphology and surface roughness of the samples were measured using AFM (Nanoscope IV multimode, digital instrument, Mikro Masch Co., USA) set to its contact mode.

The contact angle measurements on Ti and Ti-HAp matrices were measured by the sessile drop method using a contact angle meter (Digidrop, GBX Co., France), equipped with a CCD camera (25 frames/s) and a closed chamber with controlled temperature (25 ± 1°C) and relative humidity (60% RH). A drop of distilled water (3 µl) was deposited on the surface and the magnified image of its drop profile was conveyed to a computer via a CCD camera. Changes in the drop shape over time were recorded as a sequence of images that was then analyzed frame by frame with the GBX software (Windrop, GBX Co., France). For each sample, the hydrophobicity was calculated from the initial contact angle values (averaged value of contact angles measured on both sides of the drop). At least five measurements per sample were performed.

2.4 Cell culture

A HOB cell line (CCRL-11372) was cultivated to evaluate the responses of bone tissue to modified Ti matrix (Ti-HAp). Cells were plated at a seeding density of 10^5 cells/cm^2 on the sample surfaces. Dulbecco's Modified Eagle's Medium (DMEM, Gibco Co., USA) containing 10% fetal bovine serum (FBS, Gibco Co., USA), 500 unit/ml penicillin (Keunhwa Pharm Co., Korea), and 500 unit/ml streptomycin (Donga Pharm. Co., Korea) was used as media and was changed every other day. The cells were cultured at 37°C in a humidified incubator with a gas composition of 95% air and 5% CO_2.

The cytotoxicity of the matrix was evaluated by a colorimetric test using the Elizer (Spectral Max M-2, Molecular Devices Co., USA) and a lactate dehydrogenase (LDH) test [18, 19]. LDH is a cytoplasmic enzyme that leaks from the cells only upon damage of the cell membrane. The method used here is based on the determination of NADH disappearance. Briefly, after cell substrate incubation, 50 µl of the culture medium was treated with INT-tetrazolium salt. LDH that has been released from the cell catalyzes the reaction and converts INT-tetrazolium salt into a red formazan salt (A_{sample}). Also, the maximum LDH release ($A_{maximum}$) after cell lysis using 9% (v/v) Triton® X-100 and the spontaneously released LDH ($A_{spontaneous}$) in intact cells were measured. Cytotoxicity of the samples was calculated as follows:

$$\text{Cytotoxicity}(\%) = \left(A_{sample} - A_{spontaneous}\right) / \left(A_{maximum} - A_{spontaneous}\right)$$

The (3-(4,5-dimethylthiazol-2-yl)-2,5-diphenyl-tetrazolium bromide (MTT) assay is simple, accurate and yields reproducible results. Cell viability was investigated 6 days after seeding the cells using a commercially available MTT (Sigma Co., USA). Solutions of MTT, dissolved in medium or balanced salt solutions without phenol red, are yellowish in color. Mitochondrial dehydrogenases of viable cells cleave the tetrazolium ring of MTT, yielding purple formazan crystals. The standard protocol provided with the MTT kit was followed. On the 6th day after plating, 50 ml of MTT solution pre-warmed to 37°C was added in each well and cultured for 3 h. The reaction was then halted by adding 200 ml of dimethyl sulfoxide (DMSO) and 50 ml of glycin buffer into each well. Triplicate samples for each group were evaluated. The absorbance of purple formazan solution was measured at 570 nm using an ELISA plate reader (Precision Microplate Reader, Molecular Devices Co., USA) spectrophotometer. An increase or decrease in cell number resulted in a concomitant change in the amount of formazan formed, indicating the degree of cytotoxicity caused by the surfaces.

Total protein content of HOB is extremely important since it indicates healthy growth and normal cell response. In order to release the intracellular protein, the adhered cells were lysed in deionized water using a standard four-cycle freeze–thaw method. The resulting lysate solution was then used for analysis. Triplicate samples from each

group were analyzed using the Pierce BCA protein assay (Pierce Rockford Co., USA). The cell layer suspension (30 µl) was added to 200 µl of working reagent (sodium carbonate, sodium bicarbonate, BCA detection reagent, sodiumtartrate in 0.1 M NaOH, and 4% copper sulfate). The samples were incubated for 30 min at 37°C and the absorbance of the solution was measured using a spectrophotometer at a wavelength of 570 nm. The absorbance was converted to protein content using an albumin standard curve.

3 Results and discussions

3.1 FT-IR analysis of Ti-HAp matrices

The functional groups present in the samples were determined by FT-IR spectroscopy using the ATR method. Figure 1 shows the FT-IR spectra of sol–gel-derived HAp on Ti disks calcined within the temperatures range of 200 to 1400°C at 200°C intervals. The main mineral of bone, HAp exhibits absorbance resulting from the vibrational modes of phosphate and hydroxyl groups. The observed PO_4^{3-} asymmetric stretching mode of vibration is characterized by a strong complex band within the range of 1180–1000 cm^{-1} and a medium intensity band at about 975 cm^{-1} due to symmetric stretching-induced vibrations. In this respect, bands of TCP are clearly observed in the inset spectrum of Ti-HAp 800 as shown in Fig. 1. These TCP bands are different than that of HAp. The intensity of these peaks increased with an increase in calcination temperature and might be attributed to the conversion of HAp to tricalcium phosphate (TCP) and Ca–O at higher temperatures. The crystalline HAp generates characteristic OH bands at about 3400 cm^{-1}, as noticed in all the FTIR spectra. Small peaks at 1700–1450 cm^{-1} indicated the existence of a Ca–O phase in the structure.

3.2 Crystal structures of Ti-HAp matrices

The X-ray diffraction (XRD) analysis of Ti-HAp substrates is shown in Fig. 2. The X-ray spectra show Ti surface transformed into rutile when calcined at and above 800°C in the air. The broad diffraction peak observed at a low temperature of 200°C explains that the sol–gel-derived HAp is in an amorphous state. The HAp was crystallized at a higher temperature and the sizes of the crystals were increased by increasing the calcination temperature. The XRD results of HAp calcined at up to 200°C showed broad peaks of amorphous HAp (crystal plane 002) along with sharp peaks of Ti and Ti oxide (anatase) (Fig. 2). However, the HAp electrospun and calcined at 400 and 600°C exhibited crystalline phases of HAp including sharp peaks of Ti and anatase. Importantly, bioactive rutile peaks of TiO_2 are sharp and intense at and above 800°C. However, calcination above 800°C resulted in the formation of dicalcium phosphate (DCP, $Ca_2P_2O_7$), and tricalcium phosphate (TCP, $Ca_3(PO_4)_2$) due to the loss of OH groups. Nevertheless, ICP analysis and EDX (Fig. 3) showed that the weight ratio of calcium to phosphorous were 1.78 and 1.80, respectively, suggesting that sol–gel-derived HAp maintained a composition similar to that of natural bone (Ca/P; 1.67).

3.3 Morphology of heat treated Ti-HAp matrices

The surface morphology of pure Ti, Ti-HAp (sol–gel-derived) and heat treated Ti-HAp disks were studied by FE-SEM (Fig. 4) and AFM (Fig. 5). In Figs. 4 and 5, crystals can be seen to be increasing in size as the calcinations temperature is increased. Furthermore, samples

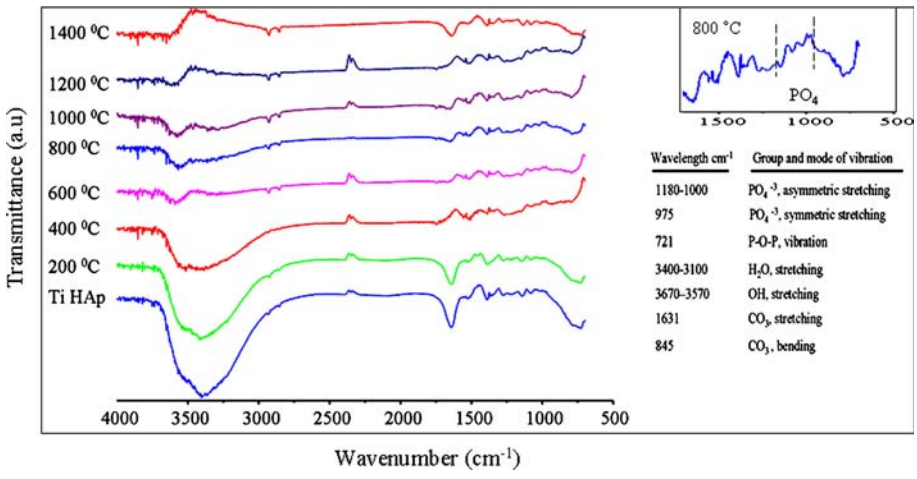

Fig. 1 FT-IR spectra of Ti-HAp matrices with (200–1400°C) and without calcinations. *Inset* at the right top is enlarged FT-IR spectrum of Ti-HAp 800 showing phosphate vibration bands

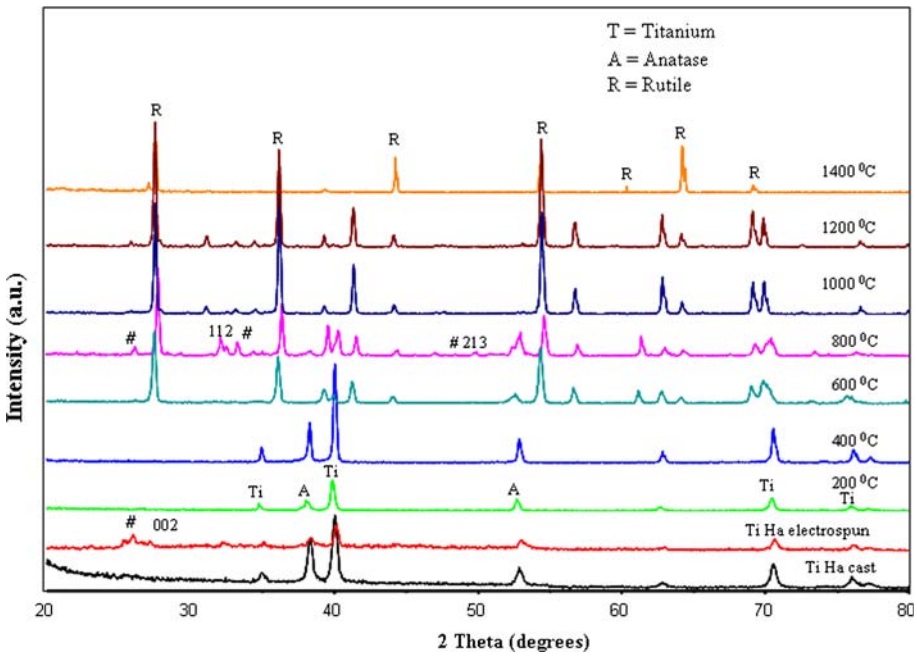

Fig. 2 X-ray diffraction patterns of Ti-HAp matrices: before and after calcination at various temperatures (200–1400°C). Symbol "#" represents the intensity peak for HAp

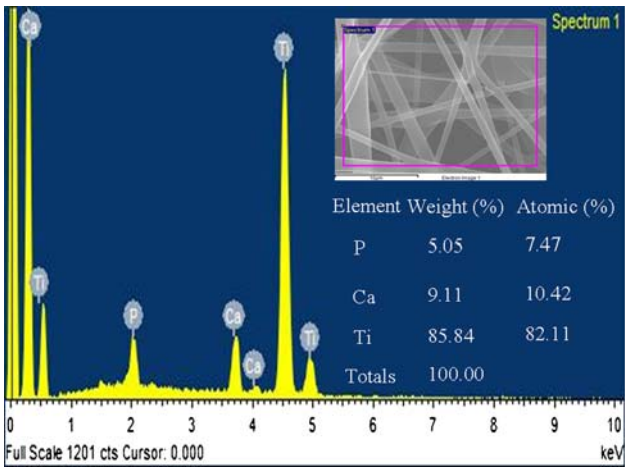

Fig. 3 EDX analysis of Ti-HAp matrix, to illustrate the elements in top electrospun layer before calcination. Ti-HAp substrate consists of TiO_2 as an inner layer and HAp as a top layer

calcined at 800°C show some rod-type crystals in addition to a predominance of hexagonal-type crystals, as reported in earlier literature [20–22]. However, the increase in crystals size corresponds to a decrease in surface area and energy at higher temperatures, especially when calcined above 1000°C. Moreover, samples calcined at 800°C were found to have well attachment of HAp on the surface of their disks. However, this was easily removed in samples calcined at and above 1200°C. This may have been caused by a loss of OH groups from $Ca(OH)_2$ resulting in the formation of CaO. It may be inferred that calcination of the Ti-HAp matrix at 800°C results in the crystalline sol–gel-derived HAp on the bioactive rutile TiO_2 favoring a well attachment of HAp on the surface. Highly crystalline surfaces have been reported to promote cell growth, and the presence of calcium ions has in the past been considered to be advantageous for such a goal [22, 23]. It is believed that the application of heat is what led to the formation of porous surfaces and the pore spaces increasing with the grain growth, caused by elevated temperatures. Also, the bioactive rutile TiO_2 is abundantly observed to be abundant at calcinations temperatures at and above 800°C. Nevertheless, we have successfully determined that surface modification method of electrospinning can foster crystal growth in a regular array, further promoting HOB cell growth.

Nevertheless, the coating thickness was reduced (136 ± 7–20 ± 2 μm) with increasing calcination temperature (200–1200°C) (Table 1). This effect may be caused by the removal of the polymer and aqueous content in the sample, which vacate the material at higher temperatures. Importantly, higher calcination temperatures also yielded an increase in the crystalline property and a reduction in thickness of the electrospun coating.

The hydrophilicity of Ti-HAp 800 was expected to vary when compared with other samples. Figure 6 shows the change of the water contact angle of Ti-HAp 800 and Ti 800 surfaces. The contact angles are 116 ± 6 and 72 ± 7 degrees for Ti 800 and Ti-HAp 800, respectively. These results are also in agreement with a previous study [24], indicating that wettability of Ti-HAp 800 was due to the outermost HAp coating formed by electrospinning. Similarly, the contact angle values of Ti-HAp samples decreased (103.4–71 degrees) with increasing calcination temperature (200–1000°C), as tabulated in the right side

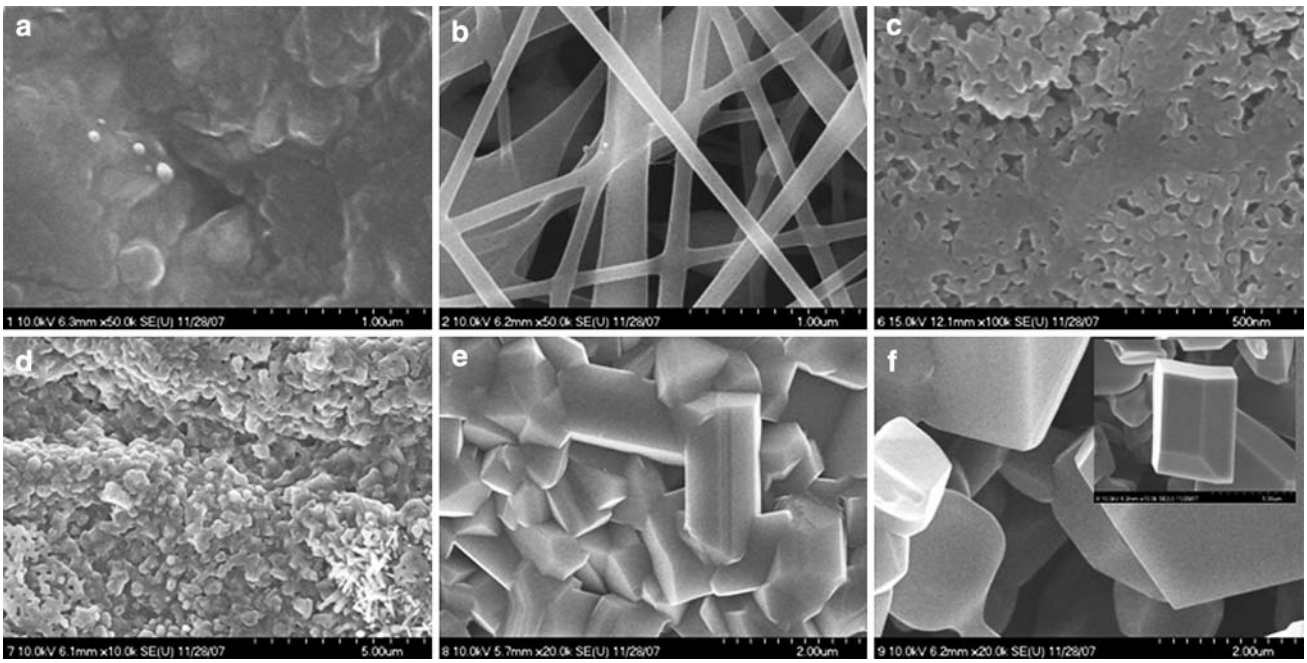

Fig. 4 FE-SEM surface images of Ti and Ti-HAp matrices: **a** the surface image of chemically etched titanium disks, **b** the electrospun disk with sol–gel derived HAp without calcination, **c–f** represents electrospun and calcined Ti-HAp matrices at 600, 800, 1000, and 1200°C, respectively

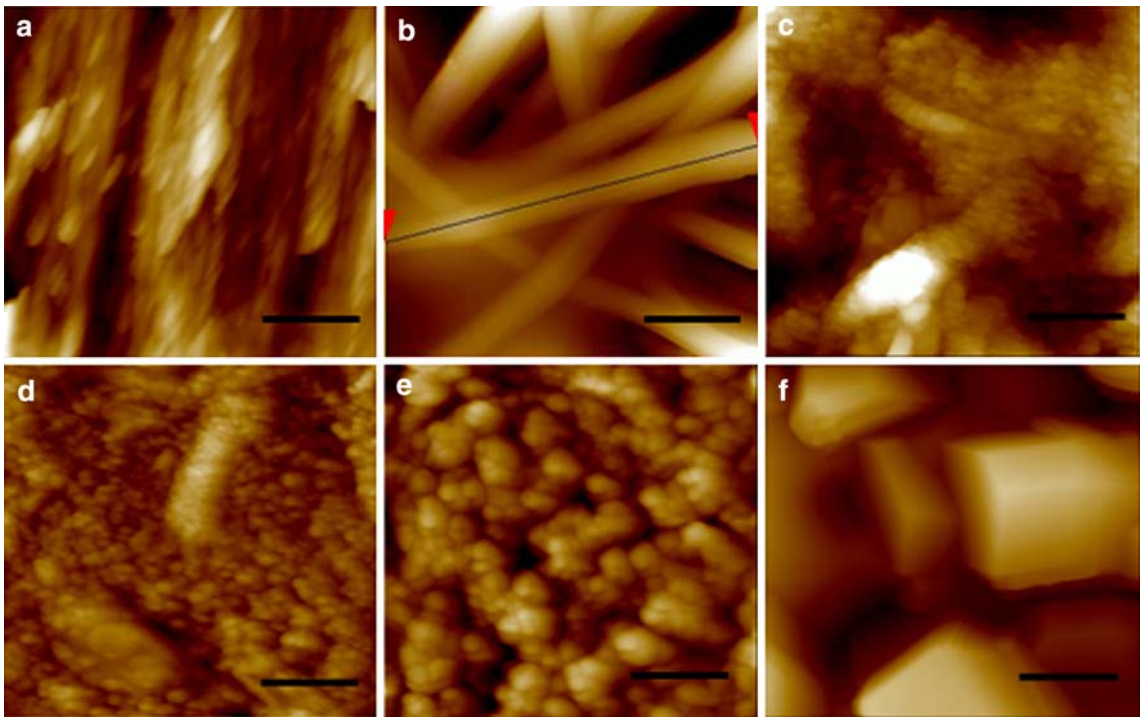

Fig. 5 AFM images of Ti and Ti-HAp matrices: **a** the surface image of chemically etched titanium disk, **b** the electrospun disk with sol–gel derived HAp, without calcination, **c–f** represents electrospun and calcined disks at 600, 800, 1000, and 1200°C, respectively. *Scale bar* represents 500 nm for all the images

of Fig. 6. However, the question remains why did such a variation in observed wettability occur? A possible answer lies in the increase in roughness of crystalline HAp due to successive calcinations, a variable property which might be responsible for the decrease in contact angle of our examined Ti-HAp samples [25].

Table 1 Roughness analysis and thickness measurement of Ti-HAp samples calcined at various temperatures

Sample	Roughness analysis by AFM (nm)				Thickness measurement by SEM (μm)
	Z range	RMS (R_q)	Mean roughness (Ra)	Maximum height (R_{max})	
Ti-HAp 200	215.6	24.9	19.6	215.6	136 ± 11
Ti-HAp 400	216.1	28.3	22.4	216.1	122 ± 7
Ti-HAp 600	321.2	44.4	34.2	321.2	62 ± 6
Ti-HAp 800	380.9	73.2	59.9	380.4	53 ± 5
Ti-HAp 1000	916.6	159.7	127.3	916.6	25 ± 3
Ti-HAp 1200	1026	196.6	162.7	1022	20 ± 2

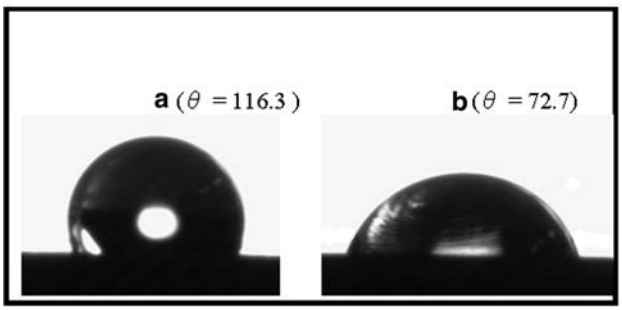

Contact angle value for various Ti-HAp samples.

Samples	Average contact Angle (θ)
Ti-HAp 200	103.4
Ti-HAp 400	92.4
Ti-HAp 600	80.6
Ti-HAp 800	72.7
Ti-HAp 1000	71

Fig. 6 Hydrophobic test with a drop of water in contact with **a** Ti 800 and **b** Ti-HAp 800. List at the right side shows the contact angle values of various Ti-HAp matrices

3.4 Cell culture

Surface chemistry and surface topography have an important influence on the performance of bone implants. Microscale surface topography can improve implant fixation mainly through mechanical interlocking. This surface architecture can profoundly affect the behaviors of cells. In this respect, we have tabulated the roughness values for various Ti-HAp samples in Table 1. As shown in Table 1, Z range values increased from 215.6 to 1026 nm with the increase in calcination temperature from 200 to 1200°C. Similarly, RMS (Rq, 24.9–196.6 nm), mean roughness (R_a, 19.6–162.7 nm) and maximum height (R_{max}, 215.6–1022 nm) values also increased with an increase in calcination temperature. Then it remains to be determined whether it is the surface chemistry or roughness that influences or provokes the promotion of a cellular response. Actually both the factors are believed to be important parameters for such guidance.

Morphology of HOB cultured for 1, 2, and 6 days on Ti and Ti-HAp surfaces is presented by FESEM (Fig. 7). Most of the cells examined were flattened, polygonally shaped and showed evidence of spreading, as well as numerous, highly extended filipodia with apparent inter cellular communication. After 6 days of culture, the HOB showed a polygonal morphology on Ti surfaces, however spreading is seen to be highest on Ti-HAp calcined at 800°C (Fig. 7i). These results indicate that the HOB are able to spread faster on Ti-HAp 800 surfaces compared to other samples (controlled Ti and Ti-HAp 600) within 6 days of culture. These cells spreading behavior seems to help the cell anchor itself to the Ti-HAp crystals, particularly those that are rod-shaped.

To ascertain the long term cytotoxic effects of Ti and Ti-HAp matrices, osteoblasts were cultured up to 6 days. HOB without a sample matrix was used as our control. The LDH assay was used to compare the extent of cell membrane disruption in the presence of various samples [26, 27]. Neither Ti nor Ti-HAp matrices induced significance damage to the cell membrane (Fig. 8). All the samples exhibited similar absorbance showing no toxicity with HOB proliferation. However, all the samples (Ti and Ti-HAp) showed slightly lower cell disruption than the control.

Similarly, HOB proliferation was seen to increase on all samples scaffolds from 1 to 6 days as evaluated by an MTT test. The results indicate an increase in the number of cells present on Ti-HAp 800 surfaces compared to the control Ti surfaces after 6 days of culture. In addition, Fig. 9 shows that the number of cells on Ti-HAp samples is higher than on the control Ti. Our results indicate that cells adhere and spread more extensively on the Ti-HAp 800 surface than on the other surfaces examined. Protein production,

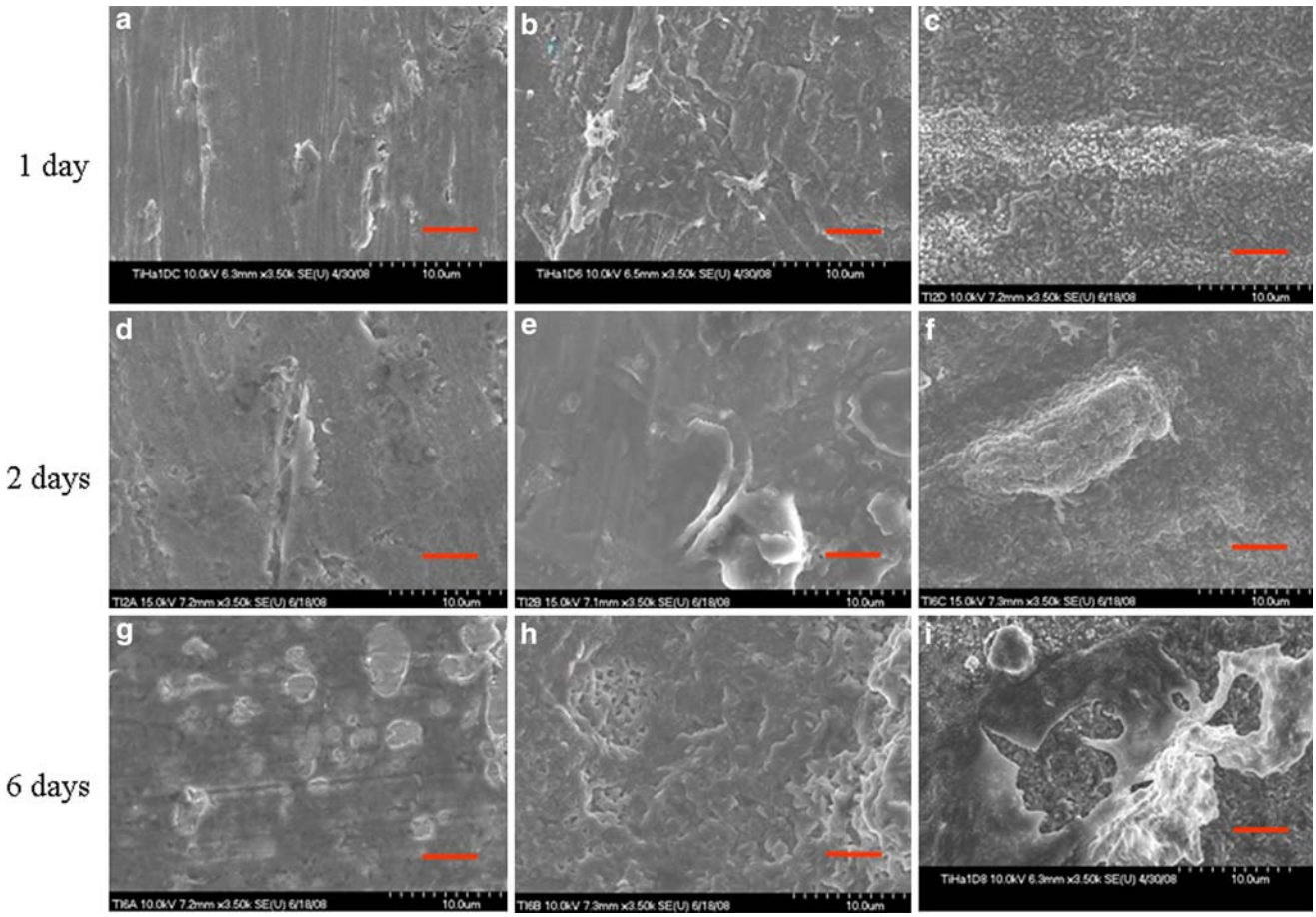

Fig. 7 FE-SEM micrographs of HOB cultured on Ti-HAp surfaces in six well plates after one (**a–c** Ti, Ti-HAp 600, and Ti-HAp 800), two (**d–f** Ti, Ti-HAp 600, and Ti-HAp 800), and six (**g–i** Ti, Ti-HAp 600, and Ti-HAp 800) days. *Scale bar* represents 5 μm

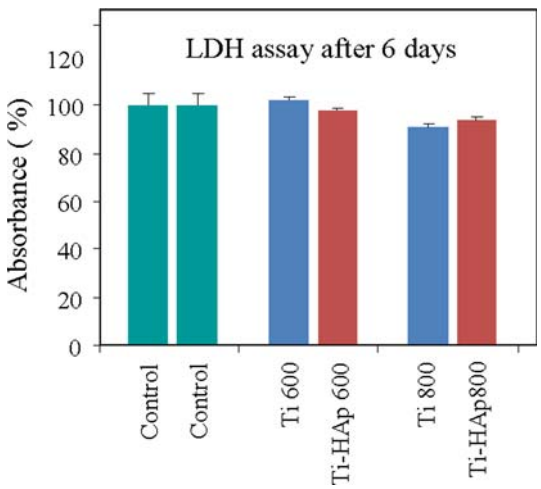

Fig. 8 Cytotoxicity evaluation on Ti and Ti-HAp matrices by LDH test after 6 days HOB culture

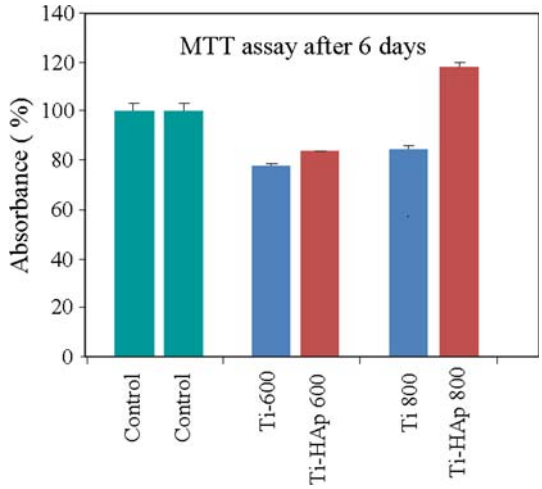

Fig. 9 Viability evaluation on Ti and Ti-HAp matrices by MTT test after 6 days HOB culture

an important marker for evaluating cell function, has been reported to play a crucial role in the calcification and architectural construction of hard tissues. In our in vitro study, it was observed that protein production was significantly increased over the 6 day incubation period. In this experiment, HOB seeded on Ti-HAp 800 produced the

higher amount (0.097 mg/ml) of protein than that of both the control Ti (0.068 mg/ml) and the Ti-HAp 600 (0.086 mg/ml). These results are consistent with the LDH and MTT results, as described previously.

The morphologic appearance of the osteoblast cells on Ti-HAp 800 surfaces was similar to that of our control surfaces. Osteoblast cells on Ti-HAp 800 surfaces were observed to be flattened and polygonal in shape. After 6 days, the cells cultured on all groups were observed to be confluent and to exhibit multilayer proliferation.

In addition, visual inspection of the matrix with finger scratching shows the stability of HAp on calcined Ti disks. It is possible that the TiO_2 layer might bind calcium and phosphate similar to the case of titanate (as infusible mass of $CaTiO_3$), but uncovering the mechanism that produces this result requires further study. Additionally, the phenomenon can be explained on the following basis: firstly, osteoblasts have a special affinity for HAp; secondly, three-dimensional structures with large specific surface area might enhance HOB proliferation. In addition, the developed porosity in the matrix makes the layer more homogeneous and crystalline, enhancing the bioactivity of the composite material. The best results in our samples, found on Ti-HAp 800, might be due to this high porosity and high surface energy of electrospun HAp, along with the bioactive rutile TiO_2 layer on the surface of the calcined samples.

4 Conclusions

This study highlighted the surface modification of Ti disks with sol–gel-derived HAp via electrospinning, resulting in a hierarchal structure. The composite matrix thus obtained is found to have a superior topographical structure to former surface modification efforts in its promotion of HOB proliferation. This finding would add a new dimension to the surface modification of implant materials to create an appropriate environment for growth and differentiation of cells.

Acknowledgments This research was supported by the Korean Research Foundation (KRF2007-211-D00032, Korean Government Project No. 10028211), Grant Funded by the Korean Government (MOEHRD), and Regional Research Centers Program of the Korean Ministry of Educational and Human Resources Development through the Center for Healthcare Technology Development, Chonbuk National University, Jeonju 562-756, Republic of Korea.

References

1. Hala ZC, Rolfe H. Titanium substrata composition influences osteoblastic phenotype: in vitro study. J Biomed Mater Res. 1999;47:360–6.
2. Garcia-Alonso MC, Saldana L, Vallés G, Gonzalez-Carrasco JL, González-Cabrero J, Martínez ME, et al. In vitro corrosion behaviour and osteoblast response of thermally oxidized Ti_6Al_4V alloy. Biomaterials. 2003;24:19–26.
3. Bidez MW, Misch CE. Force transfer in implant dentistry: basic concepts and principles. J Oral Implantol. 1992;18:264–74.
4. Im KH, Lee SB, Kim KM, Lee YK. Improvement of bonding strength to titanium surface by sol–gel derived hybrid coating of hydroxyapatite and titania by sol–gel process. Surf Coat Technol. 2007;202:1135–8.
5. Michael MC. Dental implant materials: commercially pure titanium and titanium alloys. J Prosthodont. 1999;l8:40–3.
6. Fujibayashi S, Masashi N, Kim HM, Kokubo T, Nakamura T. Osteoinduction of porous bioactive titanium metal. Biomaterials. 2004;25:443–50.
7. Kasemo B, Lausmaa J. Biomaterial and implant surface: a surface science approach. Int J Oral Maxillofac Implants. 1988;3:247–59.
8. Xuanyong L, Paul KC, Chuanxian D. Surface modification of titanium, titanium alloys, and related materials for biomedical applications. Mater Sci Eng R Rep. 2004;47:49–121.
9. Okumura M, Ohgushi H, Dohi Y, Katuda T, Tamai S, Koerten HK, et al. Osteoblastic phenotype expression on the surface of hydroxyapatite ceramics. J Biomed Mater Res. 1997;37:122–9.
10. Zhang C, Wang JX, Feng H, Lu B, Zhang X. Repairing segmental bone defects with living porous ceramic cylinders: an experimental study in dog femora. J Biomed Mater Res. 2001;55:28–32.
11. Li JP, Habibovica P, Doelc M, Wilsonb CE, Wijna JR, Clemens AV, et al. Bone ingrowth in porous titanium implants produced by 3D fiber deposition. Biomaterials. 2007;28:2810–20.
12. Kumta PN, Sfeir C, Lee DH, Olton D, Choi D. Nanostructured calcium phosphates for biomedical applications: novel synthesis and characterization. Acta Biomater. 2005;1:65–83.
13. Larsson C, Emanulesson L, Thomsen P, Ericson LE. Bone response to surface modified titanium implants—studies on the tissue response after 1 year to machined and electropolished implants with different oxide thicknesses. J Mater Sci Mater Med. 1997;8:721–9.
14. Feng B, Weng J, Yang BC, Qu SX, Zhang XD. Characterization of surface oxide films on titanium and adhesion of osteoblast. Biomaterials. 2003;24:4663–70.
15. Groessner-Schreiber B, Tuan RS. Enhanced extracellular matrix production an mineralization by osteoblasts cultured on titanium surfaces in vitro. J Cell Sci. 1992;101:209–17.
16. Barbara DB, Thomas WH, David DD, Zvi S. Role of material surfaces in regulating bone and cartilage cell response. Biomaterials. 1996;17:137–46.
17. Bajgai MP, Aryal S, Bhattarai SR, Remant Bahadur KC, Kim KW, Kim HY. Poly (ε-caprolactone) grafted dextran biodegradable electrospun matrix: a novel scaffold for tissue engineering. J Appl Polym Sci. 2008;108:1447–54.
18. Aryal S, Bajgai MP, Khil MS, Kang HS, Kim HY. Biomimetic hydroxyapatite particulate nanofiber modified silicon: in vitro bioactivity. J Biomed Mater Res. 2009;88A:384–91.
19. Hanawa T, Kamiura Y, Yamamoto S, Kohgo T, Amemiya A, Ukai H, et al. Early bone formation around calcium-ion-implanted titanium inserted into rat tibia. J Biomed Mater Res. 1997;36:131–6.
20. Li D, Ferguson SJ, Beutler T, Cochran DL, Sittig C, Hirt HP, et al. Biomechanical comparison of the sandblasted and acid etched and the machined and acid-etched titanium surface for dental implants. J Biomed Mater Res. 2002;60:325–32.
21. Frayssinet P, Tourenne F, Rouquet N, Conte P, Delga C, Bonel G. Comparative biological properties of HA plasma-sprayed coatings with different crystallinities. J Mater Sci Mater Med. 1994;5:11–7.

22. Cheung HS, McCarty DJ. Mitogenesis induced by calcium-containing crystals: role of intracellular dissolution. Exp Cell Res. 1985;157:63–70.
23. Pattanayak DK, Divya P, Upadhyay S, Prasad RC, Rao BT, Rama Mohan TR. Synthesis and evaluation of hydroxyapatite ceramics. Trends Biomater Artif Organs. 2005;18:87–92.
24. Chen W, McCarthy TJ. Layer-by-layer deposition: a tool for polymer surface modification. Macromolecules. 1997;30:78–86.
25. Stevens N, Priest CI, Sedev R, Ralston J. Wettability of photo-responsive titanium dioxide surfaces. Langmuir. 2003;19:3272–5.
26. Vihola H, Laukkanen A, Valtola L, Tenhu H, Hirvonen J. Cytotoxicity of thermosensitive polymers poly(*N*-isopropylacrylamide), poly(*N*-vinylcaprolactam) and amphiphilically modified poly-(*N*-vinylcaprolactam). Biomaterials. 2005;26:3055–64.
27. Groot K, Geesink R, Klein C, Serekian P. Plasma-sprayed coatings of hydroxyl apatite. J Biomed Mater Res. 1987;21:1375–81.